Chinese Chemical Letters 33 (2022) 1493–1496

Contents lists available at ScienceDirect

Chinese Chemical Letters

journal homepage: www.elsevier.com/locate/cclet

# Fluorescence detection of perfluorooctane sulfonate in water employing a tetraphenylethylene-derived dual macrocycle BowtieCyclophane

Sheng-Nan Lei, Huan Cong*

*Key Laboratory of Photochemical Conversion and Optoelectronic Materials, Technical Institute of Physics and Chemistry & School of Future Technology, University of Chinese Academy of Sciences, Chinese Academy of Sciences, Beijing 100190, China*

ARTICLE INFO

*Article history:*
Received 17 June 2021
Revised 10 August 2021
Accepted 13 August 2021
Available online 19 August 2021

*Keywords:*
Fluorescence
Aggregation
Perfluorooctane sulfonate
Tetraphenylethylene
Macrocycle

ABSTRACT

Because the widely used perfluorooctane sulfonate (PFOS) is harmful to both environment and human health, it is of great significance and urgency to develop sensitive and selective sensors for the detection of trace PFOS in water. In this study, a tetraphenylethylene-derived macrocycle BowtieCyclophane has been developed as a fluorescent sensor based on aggregation-induced emission enhancement and fluorochromism. Sensitive detection of PFOS has been achieved with a limit of detection (LOD) of 47.3 ± 2.0 nmol/L (25.4 ± 1.1 μg/L) accompanied by visual fluorescence color changes.



Per- and poly-fluoroalkyl substances (PFAS) have been extensively employed in consumer product manufacture and industrial processes [1,2]. Due to their exceptional stability in natural environment, PFAS have emerged as global persistent organic pollutants [3–5]. As one of the most commonly used PFAS, perfluorooctane sulfonate (PFOS) is found in natural water body worldwide, even in human blood and breast milk samples. PFOS has caused serious adverse effects for environment and health because of its toxicity and bioaccumulation [6–8]. For example, the clearance half-life of PFOS in human bodies is approximately 4 years, and PFOS is known to be relevant with fatal health issues including cancers. As a result, government policies have been strictly imposed worldwide to monitor and control the concentrations of PFOS in water under safety levels [9], which requires quick and quantitative detection methods for trace PFOS in aqueous solution.

Compared to detection techniques based on mass spectrometry or electrochemistry [10-12], fluorescence detections of PFOS in water feature low cost, facile operation, and high sensitivity [13–17]. In addition, the prosperity of aggregation induced emission (AIE) during the past twenty years has facilitated the development of AIEgen-based fluorescent sensors for various analytes [18–23], but to the best of our knowledge, quantitative detection of PFOS in water using AIE strategy has not been reported. Herein we show BowtieCyclophane (BC), a water-soluble, fluorescent macrocycle [24,25], as a novel PFOS sensor (Fig. 1). Structurally, BC is a symmetrical tetra-cationic figure-of-eight macrocycle which combines a tetraphenylethylene (TPE) core, a classic AIEgen [26–29], and pyridinium cyclophane scaffolds [30,31] on both sides. Like many TPE-derived strained macrocycles including our previously reported Bowtie Arene [32–37], aggregation of BC is accompanied by emission enhancement along with significant fluoro chromism. Such features endorse BC as an excellent fluorescence sensor for PFOS in water, achieving the limit of detection (LOD) of 47.3 ± 2.0 nmol/L (25.4 ± 1.1 μg/L) with concomitant fluorescence color change which can be easily visualized by naked-eye and quantified by smart-phone.

Starting from known building blocks tetrapyridyl TPE derivative **1** and bis(benzyl bromide) **2**, $S_N2$ reaction followed by anion exchange afforded the water-soluble macrocycle BC with high yields (Fig. 2a). Both steps were chromatography-free, and can be conducted without the need to exclude moisture and oxygen. The operationally friendly preparation secured rapid access to sufficient amount of BC. Next, various attempts to grow single crystals of BC or its hexafluorophosphate analogue **3** ended up with only fragile crystalline solids that were not well resolved by X-ray analysis. After the chloride anion was replaced by tetrakis(3,5-bis(trifluoromethyl)phenyl)borate (BArF), suitable samples for crystallographic analysis were eventually obtained, and the Bowtie-shaped tetracation of BC was unambiguously confirmed (Fig. 2b,

* Corresponding author.
*E-mail address:* hcong@mail.ipc.ac.cn (H. Cong).

https://doi.org/10.1016/j.cclet.2021.08.068
1001-8417/

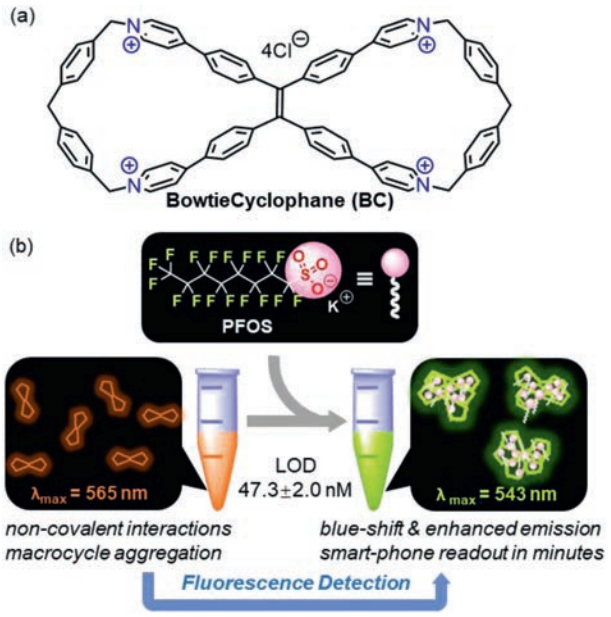


**Fig. 1.** The development of BC as a fluorescence sensor for PFOS detection.

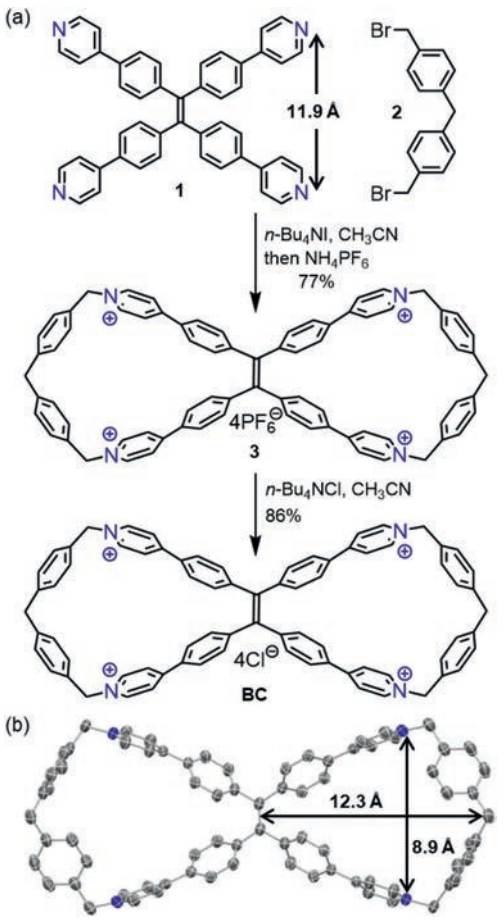


**Fig. 2.** (a) Synthesis of BC. (b) X-ray crystal structure of the BC tetracation. The hydrogen atoms and counter anions were omitted for clarity.

CCDC: 2075963). In the crystalline state, the BC displays twin cavity which extends into the bay of TPE moiety, with the rest of the cavity in the shape of a truncated pentagon. Notably, the 8.9 Å-distance between the two cationic nitrogen atoms in each cavity of BC is considerably shorter compared to the counterpart in the uncyclized precursor **1** (11.9 Å based on the reported crystal structure) [38], indicating significant macrocyclic strain within BC.

The TPE-derived strained bis-cyclic structure has endowed BC with aggregation-induced, switchable fluorescence intensity and fluorochromism (Fig. 3a). Specifically, examination of the photophysical properties of BC in a range of $H_2O$/THF mixed solvents showed constant orange emission in dilute solutions when the THF (a poor solvent for BC) contents were no higher than 80%. As the THF faction increased to 90%, an apparent fluorescence enhancement with distinct blue shift ($\Delta\lambda_{max} = 46$ nm) were observed, and the solution became opaque at the same time (Fig. S8 in Supporting information). The formation of aggregates of BC in the 10:90 $H_2O$/THF sample was confirmed by the positive Tyndall effect as well as dynamic light scattering (DLS) results (Fig. S9 in Supporting information). While the fluorescence color of BC barely changed when the THF content further reached 99%, the emission intensity exhibited another 2-fold increase which was in accordance with the observation of larger aggregates employing DLS analysis accompanied by stronger Tyndall effect (Fig. S11 in Supporting information).

The addition of PFOS could also lead to the aggregation of BC along with significant emission enhancement with evident fluorochromism from orange to bright yellow (Fig. 3b, $\Delta\lambda_{max} = 22$ nm), which was consistent with the observation of aggregates based on DLS, Tyndall effect, and SEM (Figs. S13 and S14 in Supporting information). UV-vis titration experiments indicated a stoichiometric ratio of 1:4 for BC and PFOS (Fig. S15 in Supporting information). Because the observed stoichiometry for BC and PFOS matches their intrinsic charges, we proposed that upon mixing BC and PFOS in water, anion exchange would occur to replace the chloride ions of BC with the monoanionic PFOS. As a result, the aggregation process, with concurrent emission enhancement, would be triggered by the decreased water solubility after the anion exchange from the original water-soluble chloride to the organic sulfonate (Fig. S17 in Supporting information). The long hydrophobic tail of PFOS may further facilitate the aggregation with BC through tangling or threading. These experimental observations are in consistent with previous studies which showed that the anionic head and perfluoroalkyl tail of PFOS make both ends of this linear molecule capable to interact non-covalently with cationic macrocycles through electrostatic and hydrophobic effects, respectively [16,39–41]. In addition, an apparent association constant [42] of $(1.95 \pm 0.14) \times 10^7$ L/mol was calculated for BC and PFOS based on the concentration of pyridinium units (Fig. S16 in Supporting information).

The aggregation-induced fluorochromism of BC prompted the direct comparisons of PFOS and analogous analytes under a range of concentrations by naked-eye visualization (Fig. 4a). Under the irradiation of 365 nm UV light, fluorescence color changes emerged for perfluorobutyl sulfonate at the concentration as low as $10^{-6}$ mol/L, which is two orders of magnitude more sensitive than the corresponding carboxylate (*n*-$C_4F_9SO_3K$ *vs.* *n*-$C_4F_9CO_2K$). Moreover, the minimum concentrations for visualizable changes were similarly at $10^{-6}$ mol/L for perfluoroalkyl sulfonates bearing $C_{4+}$ chains (*n*-$C_4F_9SO_3K$, *n*-$C_6F_{13}SO_3K$ and *n*-$C_8F_{17}SO_3K$), while the trifluoromethyl, phenyl, *n*-butyl, and methyl sulfonates exhibited inferior sensitivity. The above results demonstrate the excellent specificity for PFOS detection based on the highly responsive fluorescence changes of BC.

Next, a quantification assay for trace amount of PFOS was investigated. When the PFOS-induced fluorochromism of BC was mapped onto the 1931 CIE chromaticity diagram (Fig. S20 in Supporting information), the emissions were found blue-shifted at low PFOS concentrations. Therefore, real-time quantification of PFOS

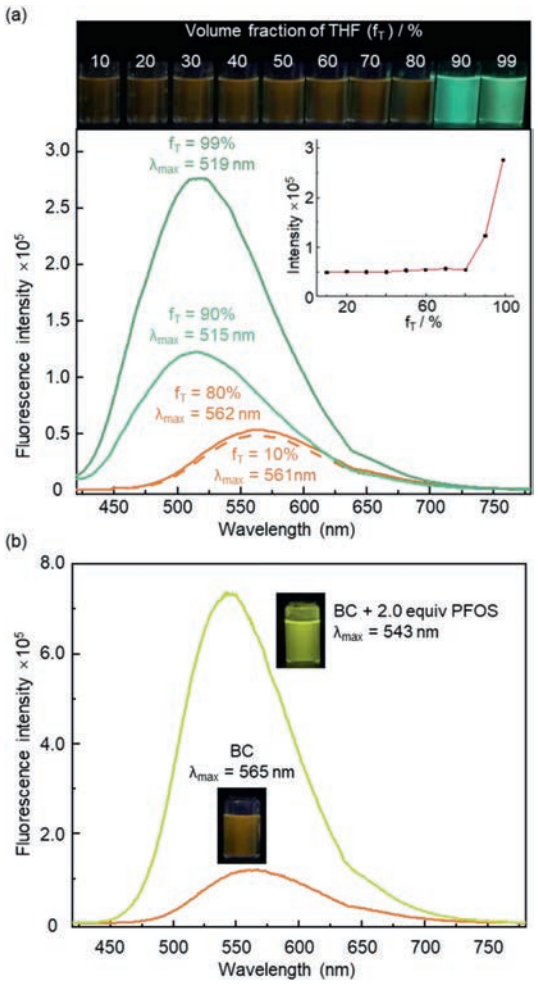


**Fig. 3.** (a) Pictures (under 365 nm UV light) and fluorescence spectra of BC ($2.0 \times 10^{-5}$ mol/L, $\lambda_{ex}$ = 400 nm) in $H_2O$/THF mixed solvents (inset) Plot of maximum emission intensities against volume fractions of THF. (b) Fluorescence spectra of BC ($2.0 \times 10^{-5}$ mol/L in water, $\lambda_{ex}$ = 400 nm) before and after the addition of PFOS.

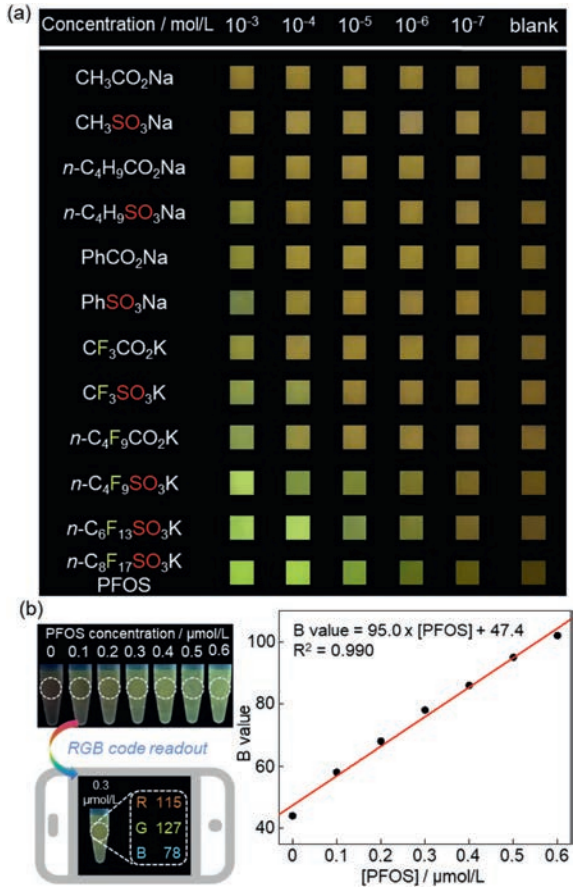


**Fig. 4.** (a) Visualizable fluorochromism of BC in response to PFOS and analogous analytes under different concentrations (irradiated by 365 nm UV light). (b) Real-time quantification of PFOS using the fluorochromism assay of BC with a smartphone (irradiated by 365 nm UV light).

can be achieved using a smart-phone within minutes [43,44] according to the following simple protocols (Fig. 4b): (1) mixing stock solutions of PFOS and BC (total volume of 1.0 mL, with BC concentration of $1.0 \times 10^{-6}$ mol/L) in each 2 mL plastic centrifuge vial, and shaking the mixture for 30 s; (2) taking a photo of each sample under 365 nm UV irradiation; (3) analyzing the photos with a phone App to extract the GRB coordinates. Next, the resulting blue color codes (B values) of the samples were plotted against the PFOS concentrations, and the calibration curve established linear correlations within the 0 to 0.6 μmol/L range of PFOS.

Moreover, analyzing the relative fluorescence intensity under different PFOS concentrations also indicated a linear calibration curve with the LOD value of 47.3 ± 2.0 nmol/L (25.4 ± 1.1 μg/L) by the $3\sigma$/slope method (Fig. 5a) [45]. The specificity of the PFOS detection using BC was evaluated by addition of excess common interfering species (100-fold concentration relative to BC), which led to minor fluorescence quenching of BC in the absence of PFOS (Fig. 5b, gray bars). Additionally, the emission enhancement of BC remained highly sensitive to PFOS in the presence of these competing cations or anions (Fig. 5b, blue bars). We further evaluated the performance of the fluorescence intensity assay using tap water, which was directly used without pre-treatment prior to addition of PFOS. An LOD value of 77.8 ± 8.8 nmol/L (41.9 ± 4.9 μg/L) was determined (Fig. S22 in Supporting information). These data demonstrated the excellent selectivity and robustness of the BC-based fluorescent detection method.

In summary, a figure-of-eight water-soluble macrocycle BC have been developed as the first AIE-based macrocyclic fluorescence sensor for PFOS detection in aqueous solution. The addition of PFOS can induce aggregation of BC thereby trigger significant changes in both fluorescence intensity and color. The fluorochromism-based PFOS detection is visualisable and quantifiable using a smart-phone. The fluorescence intensity assay features low LOD and high specificity. Further investigation of BC and other strained fluorescent macrocycles are underway and will be reported in due course.

## Declaration of competing interest

The authors declare that they have no known competing financial interests or personal relationships that could have appeared to influence the work reported in this paper.

## Acknowledgments

Financial support from the National Natural Science Foundation of China (Nos. 21672227, 21922113, 22071257), the Strategic Priority Research Program of Chinese Academy of Sciences (No. XDB17000000), the National Key Research and Development Program of China (No. 2017YFA0206903), K. C. Wong Education Foundation, and the TIPC Director's Fund is gratefully acknowledged. We thank Prof. Congyang Wang (ICCAS), Drs. Xiaodi Yang (Shanghai

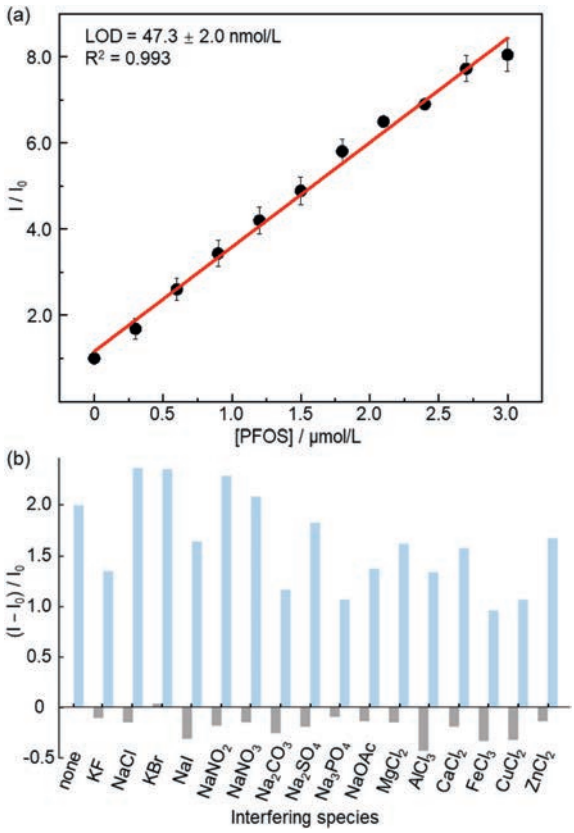


**Fig. 5.** (a) Quantification of PFOS using the relative fluorescence intensity assay of BC ($1.0 \times 10^{-6}$ mol/L in water, $\lambda_{ex}$ = 400 nm, at 25 °C). Error bars represent mean ± s.d. (three duplicate experiments). (b) Fluorescence intensity of BC ($1.0 \times 10^{-6}$ mol/L in water, $\lambda_{ex}$ = 400 nm, at 25 °C) upon addition of interfering species (100 equiv. to BC, grey bars), followed by addition of PFOS (1 equiv. to BC, blue bars).

University of Traditional Chinese Medicine), Jie Su and Wen Zhou (Peking University) for the help with compound characterizations. Dr. Li Ren (China Jiliang University), Dr. Liu-Pan Yang (Southern University of Science and Technology), Ms. Xiao-Xiao Hu (TIPCCAS) are acknowledged for helpful discussions and experimental assistance.

## Supplementary materials

Supplementary material associated with this article can be found, in the online version, at doi:10.1016/j.cclet.2021.08.068.

## References

[1] Z. Wang, I.T. Cousins, M. Scheringer, R.C. Buck, K. Hungerbühler, Environ. Int. 69 (2014) 166–176.
[2] Z. Wang, J.C. DeWitt, C.P. Higgins, I.T. Cousins, Environ. Sci. Technol. 51 (2017) 2508–2518.
[3] K.A. Barzen-Hanson, J.A. Field, Environ. Sci. Technol. Lett. 2 (2015) 95–99.
[4] K.T. Trenck, R. Konietzka, A. Biegel–Engler, et al., Environ. Sci. Eur. 30 (2018) 19.
[5] L. Liu, Y. Qu, J. Huang, R. Weber, Environ. Sci. Eur. 33 (2021) 6.
[6] M.S. Johnson, R.C. Buck, I.T. Cousins, C.P. Weis, S.E. Fenton, Environ. Toxicol. Chem. 40 (2021) 543–549.
[7] A.O.D. Silva, J.M. Armitage, T.A. Bruton, et al., Environ. Toxicol. Chem. 40 (2021) 631–657.
[8] K. Steenland, A. Winquist, Environ. Res. 194 (2021) 110690.
[9] U.S. Environmental Protection Agency, PFAS Action Plan: Program Update (February 2020) www.epa.gov/pfas/pfas-action-plan-program-update-february-2020.
[10] M.A. Amin, Z. Sobhani, Y. Liu, et al., Environ. Technol. Innov. 19 (2020) 100879.
[11] K. Gao, Y. Chen, Q. Xue, et al., Trends Analyt. Chem. 133 (2020) 116114.
[12] H. Ryu, B. Li, S.D. Guise, J. McCutcheon, Y. Lei, J. Hazard. Mater. 408 (2021) 124437.
[13] J. Liang, X. Deng, K. Tan, Spectrochim. Acta A: Mol. Biomol. Spectrosc. 150 (2015) 772–777.
[14] C. Fang, X. Zhang, Z. Dong, et al., Chemosphere 191 (2018) 381–388.
[15] C. Fang, J. Wu, Z. Sobhani, M.A. Amin, Y. Tang, Anal. Methods 11 (2019) 163–170.
[16] Z. Zheng, H. Yu, W.C. Geng, et al., Nat. Commun. 10 (2019) 5762.
[17] R.F. Menger, E. Funk, C.S. Henry, T. Borch, Chem. Eng. J. 417 (2021) 129133.
[18] D.D. La, S.V. Bhosale, L.A. Jones, S.V. Bhosale, ACS Appl. Mater. Interfaces 10 (2018) 12189–12216.
[19] M. Gao, B.Z. Tang, ACS Sens. 2 (2017) 1382–1399.
[20] Y. Xie, Z. Li, Chem. Asian J. 14 (2019) 2524–2541.
[21] J.G. Yu, L.Y. Sun, C. Wang, Y. Li, Y.F. Han, Chem. Eur. J. 27 (2021) 1556–1575.
[22] A. Feng, F. Jiang, G. Huang, P. Liu, Spectrochim. Acta A: Mol. Biomol. Spectrosc. 224 (2020) 117446.
[23] H. Wan, Q. Xu, P. Gu, et al., J. Hazard. Mater. 403 (2021) 123656.
[24] T.L. Mako, J.M. Racicot, M. Levine, Chem. Rev. 119 (2019) 322–477.
[25] C. Guo, A.C. Sedgwick, T. Hirao, J.L. Sessler, Coord. Chem. Rev. 427 (2021) 213560.
[26] J. Mei, N.L.C. Leung, R.T.K. Kwok, J.W.Y. Lam, B.Z. Tang, Chem. Rev. 115 (2015) 11718–11940.
[27] X. Cai, B. Liu, Angew. Chem. Int. Ed. 59 (2020) 9868–9886.
[28] H. Wan, Q. Xu, P. Gu, et al., J. Hazard. Mater. 403 (2021) 123656.
[29] L. Dong, H.Q. Peng, L.Y. Niu, Q.Z. Yang, Top Curr. Chem. 379 (2021) 18.
[30] Z. Liu, S.K.M. Nalluri, J.F. Stoddart, Chem. Soc. Rev. 46 (2017) 2459–2478.
[31] I. Neira, A. Blanco-Gómez, J.M. Quintela, M.D. García, C. Peinador, Acc. Chem. Res. 53 (2020) 2336–2346.
[32] H.T. Feng, Y.X. Yuan, J.B. Xiong, Y.S. Zheng, B.Z. Tang, Chem. Soc. Rev. 47 (2018) 7452–7476.
[33] Y. Liu, F.X. Lin, Y. Feng, et al., ACS Appl. Mater. Interfaces 11 (2019) 34232–34240.
[34] Y. Li, Y. Dong, L. Cheng, et al., J. Am. Chem. Soc. 141 (2019) 8412–8415.
[35] H. Nian, A. Li, Y. Li, et al., Chem. Commun. 56 (2020) 3195–3198.
[36] S.N. Lei, H. Xiao, Y. Zeng, et al., Angew. Chem. Int. Ed. 59 (2020) 10059–10065.
[37] K. Teng, Q. Yang, Chin. J. Org. Chem. 40 (2020) 549–550.
[38] G. Huang, G. Zhang, D. Zhang, Chem. Commun. 48 (2012) 7504–7506.
[39] L. Xiao, Y. Ling, A. Alsbaiee, et al., J. Am. Chem. Soc. 139 (2017) 7689–7692.
[40] H. Omorodion, M. Palenzuela, M. Ruether, et al., New J. Chem. 42 (42) (2018) 7956–7968.
[41] M.J. Klemes, Y. Ling, C. Ching, et al., Angew. Chem. Int. Ed. 58 (2019) 12049–12053.
[42] L.J. Chen, S.J. Humphrey, J.L. Zhu, et al., J. Am. Chem. Soc. 143 (2021) 8295–8304.
[43] L. Han, Y.Z. Fan, M. Qing, et al., ACS Appl. Mater. Interfaces 12 (2020) 47099–47107.
[44] L. Jia, R. Chen, J. Xu, et al., J. Hazard. Mater. 413 (2021) 125296.
[45] D. MacDougall, W.B. Crummett, Anal. Chem. 52 (2002) 2242–2249.